J Physiol 586.23 (2008) pp 5665–5678

The Journal of Physiology

GABA transporter 1 tunes GABAergic synaptic transmission at output neurons of the mouse neostriatum

Knut Kirmse, Anton Dvorzhak, Sergei Kirischuk and Rosemarie Grantyn

Institute of Neurophysiology, Johannes Müller Centre of Physiology, Charité – University Medicine Berlin, Berlin, Germany

GABAergic medium-sized striatal output neurons (SONs) provide the principal output for the neostriatum. *In vitro* and *in vivo* data indicate that spike discharge of SONs is tightly controlled by effective synaptic inhibition. Although phasic GABAergic transmission critically depends on ambient GABA levels, the role of GABA transporters (GATs) in neostriatal GABAergic synaptic transmission is largely unknown. In the present study we aimed at elucidating the role of GAT-1 in the developing mouse neostriatum (postnatal day (P) 7–34). We recorded GABAergic postsynaptic currents (PSCs) using the whole-cell patch-clamp technique. Based on the effects of NO-711, a specific GAT-1 blocker, we demonstrate that GAT-1 is operative at this age and influences GABAergic synaptic transmission by presynaptic and postsynaptic mechanisms. Presynaptic $GABA_BR$-mediated suppression of GABA release was found to be functional at all ages tested; however, there was no evidence for persistent $GABA_BR$ activity under control conditions, unless GAT-1 was blocked (P12–34). In addition, whereas no tonic $GABA_AR$-mediated conductances were detected in SONs until P14, application of a specific $GABA_AR$ antagonist caused distinct tonic outward currents later in development (P19–34). In the presence of NO-711, tonic $GABA_AR$-mediated currents were also observed at P7–14 and were dramatically increased at more mature stages. Furthermore, GAT-1 block reduced the median amplitude of GABAergic miniature PSCs indicating a decrease in quantal size. We conclude that in the murine neostriatum GAT-1 operates in a net uptake mode. It prevents the persistent activation of presynaptic $GABA_BRs$ (P12–34) and prevents (P7–14) or reduces (P19–34) tonic postsynaptic $GABA_AR$ activity.

(Resubmitted 20 August 2008; accepted after revision 30 September 2008; first published online 2 October 2008)
Corresponding author K. Kirmse: Institute of Neurophysiology, Johannes Müller Centre of Physiology, Charité – University Medicine Berlin, Tucholskystr. 2, 10117 Berlin, Germany. Email: knut.kirmse@charite.de

Within the basal ganglia complex the (neo)striatum represents the principal input structure and plays a decisive role in cognitive tasks and execution of movement (for review see Gerfen, 1992; Balleine *et al.* 2007). Most neurons in the striatum (about 95%, for review see Tepper *et al.* 2008) are GABAergic medium-sized striatal output neurons (SONs). They receive excitatory afferents from the cerebral cortex and thalamus, and in adult animals glutamatergic contacts clearly outnumber GABAergic synapses at SONs (Hattori & McGeer, 1973; Ingham *et al.* 1998). However, as in other parts of the brain, maturation of GABAergic synaptic signalling precedes that of glutamatergic inputs. Whereas the phase of most intense glutamatergic synaptogenesis occurs during the third postnatal week (in rodents), symmetric synapses appear morphologically mature by the end of the second postnatal week, and their density changes little during the following weeks of life (Tepper *et al.* 1998; Uryu *et al.* 1999). This developmental profile is also corroborated by electrophysiological data (Misgeld *et al.* 1986; Tepper *et al.* 1998).

Until what age, and if at all, GABA plays the role of an excitatory neurotransmitter in the striatum is not yet clear (see Bracci & Panzeri, 2006). But in the adult striatum GABAergic synapses effectively control the level of striatal output activity by exerting inhibition. For example, local application of a $GABA_A$ receptor blocker *in vivo* increased the spontaneous firing rate of striatal neurons by $> 300\%$ (Nisenbaum & Berger, 1992). At the behavioural level, a disruption of striatal GABAergic signalling has been shown to severely perturb locomotor and postural functions (Yoshida *et al.* 1991; Yamada *et al.* 1995). The vast majority of GABAergic synapses on SONs originate from different classes of GABAergic interneurons and axon collaterals of SONs themselves (for review see Kawaguchi *et al.* 1995; Tepper *et al.* 2008) producing feed-forward and feed-back inhibition, respectively. It has

This paper has online supplemental material.

DOI: 10.1113/jphysiol.2008.161943

been relevant for the selection of animal age in the present study that fast-spiking (FS) interneurons (a subpopulation of GABAergic interneurons comprising < 1% of striatal neurons) mature earlier than SONs, both in anatomical and in functional terms (Tepper *et al.* 1998; Plotkin *et al.* 2005). Two weeks postnatally, i.e. before/during the formation of glutamatergic cortico-striatal synapses, GABAergic interneurons can be assumed to represent the principal GABAergic input to SONs.

Acting via ionotropic ($GABA_A$, $GABA_C$) and metabotropic ($GABA_B$) receptors, GABA can produce both phasic and tonic inhibitory currents. Both types of action critically depend on the level of ambient GABA, which in turn is mainly regulated via high-affinity GABA transporters (GATs) operating either in the forward (uptake) or reverse (release) mode (for review see Gadea & Lopez-Colome, 2001; Richerson & Wu, 2003; Cavelier *et al.* 2005). In the rodent striatum, GAT-1 is already expressed in neonates (Jursky & Nelson, 1996). In a recent study, Ade *et al.* (2008) reported that tonic $GABA_A$R-mediated conductances in SONs from postnatal day 16–25 increased after blocking GAT-1, which suggests that this transporter predominantly operates in a net uptake mode. However, no information is currently available as to what extent phasic GABAergic synaptic transmission at SONs is subject to regulation by GAT activity.

The principal aim of the present study was to elucidate whether GAT-1 shapes GABAergic synaptic transmission on SONs during a most critical period of development, when the wave of intense cortico-striatal synaptogenesis starts. Additional sets of experiments were carried out in both younger and older animals to clarify developmental changes.

Methods

Animals

Pigmented C57BL/6N wild-type mice ($n = 70$ animals, age – postnatal day (P) 7–34) were used in the present study. All experimental procedures were carried out according to the permit given by the State Office of Health and Social Affairs Berlin (Landesamt für Gesundheit und Soziales Berlin, T0121/03), which complies with international and European Union norms. Experiments were designed to minimize the number of animals used.

Preparation of brain slices

Experiments were conducted with C57BL/6N mice pups of three age groups: P7–9, P12–14 and P28–34 (the day of birth was designated as P0) – the majority of experiments being performed at P12–14. In only one set of experiments (as explicitly indicated in the text) were slices prepared from mice aged P19–21 (see Fig. 2*E–H*). Animals were decapitated under deep ether anaesthesia. The brain was removed quickly and transferred into ice-cold saline that contained (in mM): 125 NaCl, 4 KCl, 10 glucose, 1.25 NaH_2PO_4, 25 $NaHCO_3$, 0.5 $CaCl_2$ and 2.5 $MgCl_2$, constantly aerated with a 5% CO_2–95% O_2 mixture (pH 7.3). The brain was separated into two hemispheres. Coronal slices comprising the striatum of one hemisphere were cut on a vibrating microtome (Integraslice 7550PSDS, Campden Instruments Ltd, Loughborough, UK). After preparation, slices (200 μm thick) were stored for at least 1 h at room temperature in artificial cerebrospinal fluid (ACSF) that contained (in mM): 125 NaCl, 4 KCl, 10 glucose, 1.25 NaH_2PO_4, 25 $NaHCO_3$, 2 $CaCl_2$ and 1 $MgCl_2$. pH was buffered to 7.3 by continuous bubbling with a 5% CO_2–95% O_2 mixture. The osmolarity was 330 mosmol l^{-1}.

Electrophysiological recordings in acute slices

For recordings, slices were placed into a recording chamber (~0.4 ml volume) on the microscope stage (Axioscope 2 FS plus, Zeiss, Oberkochen, Germany) equipped with infrared differential interference contrast videomicroscopy. A 63× or 40× water immersion objective (Zeiss, Oberkochen, Germany) was used for cell visualization. Slices were submerged with a constant flow of oxygenated ACSF. Flow rate was set to 1–2 ml min^{-1} using a gravity-driven manually operated superfusion system. Inhibitory postsynaptic currents (IPSCs) were recorded using the whole-cell configuration of the patch-clamp technique. Intra-pipette solution contained (in mM): 100 potassium gluconate, 50 KCl, 5 NaCl, 0.5 $CaCl_2$, 5 EGTA, 25 Hepes, 2 MgATP, 0.3 GTP; pH was set to 7.2 with KOH (low Cl^- solution, calculated equilibrium potential for chloride $E_{Cl} \approx -22$ mV). The osmolarity was 320 mosmol l^{-1}. Alternatively (as indicated in the text), an intrapipette solution containing the following was used (in mM): 150 KCl, 5 NaCl, 0.5 $CaCl_2$, 5 EGTA, 25 Hepes, 4 MgATP and 0.3 GTP; pH was set to 7.2 with KOH (high Cl^- solution, $E_{Cl} \approx 4$ mV). Pipette resistance was 3–6 MΩ, when filled with the above saline. Electrophysiological signals were acquired using an EPC-8 or EPC-7 amplifier (List, Darmstadt, Germany), a 16-bit AD/DA board (ITC-16, HEKA Elektronik, Lambrecht, Germany), and TIDA 4.11 software (HEKA Elektronik, Lambrecht, Germany). The signals were filtered at 3 kHz and sampled at a rate of 10 kHz. Liquid junction potentials were not corrected. In the voltage-clamp mode the holding potential was set to –70 mV.

Access resistance was controlled by applying hyperpolarizing pulses of 10 mV from a holding potential of –70 mV. Cell capacitance and access resistance values were obtained by fitting a monoexponential function to the capacitance artefacts. Only recordings with a series

resistance below 30 MΩ were accepted (in typical cases series resistance amounted to 15–20 MΩ). In some cells series resistance compensation (50–70%) was applied. Cells exhibiting more than 20% changes in the access resistance during an experiment were discarded.

Electrical stimulation

Evoked postsynaptic currents were elicited by focal electrical stimulation through a glass pipette filled with ACSF (about 10 MΩ) and positioned in the dorsal striatum (distance between recording and stimulating electrode typically $> 100\,\mu$m). In this case, *N*-(2,6-dimethylphenylcarbamoylmethyl)-triethylammonium bromide (QX-314, 2 mM) was added to the intracellular solution to prevent generation of action potentials in the tested neurons. Paired pulses (interstimulus-interval (ISI) 50 or 250 ms) were delivered at a frequency of 0.1 Hz. An isolated stimulation unit was used to generate rectangular electrical pulses. Pulse duration was set to 0.5 ms. In the majority of experiments pulse intensity was adjusted to activate a unitary synaptic input (minimal stimulation, see Kirmse *et al.* 2007). Stimulation was accepted as minimal if the following criteria were satisfied: (1) eIPSC latency remained stable (< 20% fluctuations); (2) lowering stimulus intensity by 20% resulted in a complete failure of eIPSCs; (3) an increase in stimulus intensity by 20% changed neither mean eIPSC amplitude nor eIPSC shape. Typical pulse intensity required for minimal stimulation was between 1 and 2 μA. In some cases not all of the specified criteria were strictly met. Since results were comparable with respect to the parameters presented here, all data were pooled.

Solutions and chemicals

All experiments were performed at room temperature (22–25°C). During experiments, 10 μM 6,7-dinitro-quinoxaline-2, 3-dione (DNQX, an AMPA/kainate receptor antagonist) and 50 μM DL-2-amino-5-phosphonopentanoic acid (APV, an NMDA receptor blocker) were added to the ACSF to block glutamatergic currents. The remaining postsynaptic currents were completely blocked by bicuculline methiodide (BMI, 20 μM; see Fig. 2*A* and *E*) or SR-95531 (gabazine, 10 μM), but not strychnine (30 μM), indicating their GABAergic nature. Miniature IPSCs (mIPSCs) were recorded in the presence of tetrodotoxin (TTX, 1 μM). TTX was obtained from Alomone Laboratories (Jerusalem, Israel). 2*S*-3-[[(1*S*)-1-(3,4-Dichlorophenyl)ethyl]amino-2-hydroxypropyl](phenylmethyl)phosphinic acid (CGP55845) and SNAP-5114 were obtained from Tocris (Bristol, UK). All other chemicals were obtained from Sigma-Aldrich (Munich, Germany).

Data evaluation and statistics

All data were evaluated off-line using TIDA 4.11 (HEKA Elektronik, Lambrecht, Germany), Origin 4.10 (OriginLab Inc., Northampton, MA, USA) and SPSS 12.0 (SPSS GmbH Software, Munich, Germany). mIPSCs were analysed using PeakCount v3.2 software (C. Henneberger, Institute of Neurophysiology, Berlin). The program employs a derivative threshold-crossing algorithm to detect individual mIPSCs. Each automatically detected event is displayed for visual inspection. mIPSC rise times and decay time constants (a single exponential fit) can also be obtained. For measurement of changes in holding current (ΔI_{hold}), mean I_{hold} values were determined for consecutive 5 s periods throughout the recording. I_{hold} values were plotted and detrended by a linear fit obtained from the control segment to correct for potential steady shifts during the recording. For calculation of the bicuculline methiodide-sensitive current, we usually used the 2–4 min period that immediately preceded drug application and a 30–60 s period following about 1 min after the start of application. For illustration purposes, all-point histograms were plotted for 10 s periods of the control and test conditions, and Gaussian functions were used to fit the part of each distribution not skewed by synaptic events (see Glykys & Mody, 2007; Ade *et al.* 2008).

All results are presented as means ± S.E.M. The error bars in all figures indicate S.E.M. Unless otherwise stated, differences between means were tested for significance using a paired Student's *t* test (for pairwise comparisons) or ANOVA followed by *post hoc t* tests (for multiple comparisons). In case of small sample sizes ($n < 7$) non-parametric tests were applied (Wilcoxon's matched pairs test for two dependent samples, Mann–Whitney *U* test for two independent samples).

Results

Identification of striatal output neurons

The majority of experiments presented here have been performed in slices prepared from mice aged P12–14, with additional experiments carried out at P7–9, P19–21 and P28–34 to allow for developmental comparisons. Since most SONs acquire their spiny morphology only after the second postnatal week, we do not use the otherwise synonymous term 'medium-sized spiny neuron' (Hattori & McGeer, 1973; Chronister *et al.* 1976; Tepper *et al.* 1998). Putative SONs in the dorsal striatum were preselected according to morphological criteria, i.e. (1) medium soma size and (2) polygonal soma shape. This permitted us to distinguish SONs from large cholinergic interneurons. Cells were classified as SONs when they also met the following electrophysiological criteria (Fig. 1*A* and *B*): (1) inward rectification, (2) ramp depolarization in response

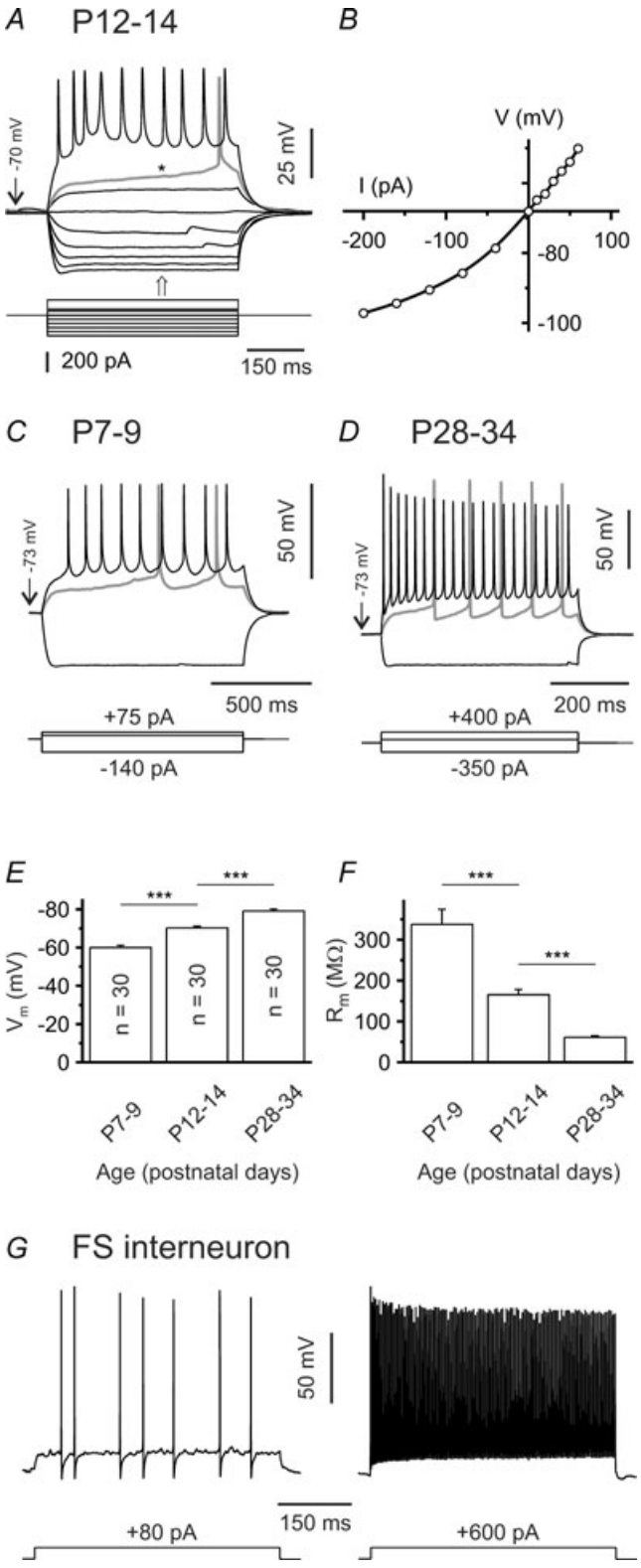

Figure 1. Electrophysiological characterization of SONs
A, sample voltage traces recorded in current-clamp mode to illustrate responses to hyperpolarizing and depolarizing current injections at P12–14. In this case QX-314 was omitted from the pipette solution. Note presence of a depolarizing ramp (*) and long latency to the first spike (> 400 ms) at juxta-threshold currents. Also note that firing frequency remained in medium range (~20 s^{-1}). *B*, current–voltage relationship for same cell as in *A*. Note inward rectification. *I–V* plot was calculated from data points at the time indicated by the arrow in *A*. *C–D*, sample voltage traces recorded in current-clamp mode to illustrate responses to hyperpolarizing and depolarizing current injections at P7–9 (*C*) and P28–34 (*D*). *E–F*, resting membrane potential (V_m, *E*) and membrane resistance (R_m, *F*) of SONs are age dependent. *G*, sample voltage traces recorded in current-clamp mode to illustrate discharge behaviour of a fast-spiking interneuron (P31) in response to depolarizing current injections of increasing amplitude. Note short spike duration, brief afterhyperpolarizations and high maximal firing frequency (> 250 s^{-1}). ***$P < 0.001$.

to juxta-threshold current injections, and (3) long latency to the first spike (if sodium channel blockers were omitted) (Kita *et al.* 1984; Nisenbaum & Wilson, 1995). Fast-spiking interneurons could be easily distinguished on the basis of their characteristic firing pattern (an example is shown in Fig. 1*G*). However, in slices prepared from young (P7–9) animals inward rectification was typically weak. Furthermore, a larger fraction of cells could not be reliably identified as belonging to one of the known striatal neuron types and were therefore not included in the analysis. Although not tested systematically, the maximum firing rate of SONs tended to increase with postnatal age (Fig. 1*A*, *C* and *D*). Resting membrane potential was measured immediately after establishing the whole-cell configuration and progressively shifted to more hyperpolarized values during postnatal life (P7–9: –60.0 ± 1.2 mV ($n = 30$), P12–14: –70.2 ± 0.9 mV ($n = 30$), P28–34: –79.1 ± 1.0 mV ($n = 30$); $P < 0.001$; Fig. 1*E*). Note, however, that these values were not corrected for seal and input resistance as proposed by Tyzio *et al.* (2003). The membrane resistance declined considerably during the same time period (P7–9: 337.7 ± 36.7 MΩ ($n = 30$), P12–14: 165.6 ± 12.8 MΩ ($n = 30$), P28–34: 61.2 ± 3.9 MΩ ($n = 30$); $P < 0.001$, ANOVA followed by *post hoc* Tamhane-T2 test for unequal group variances; Fig. 1*F*).

Since SONs projecting to the pallidum and to the substantia nigra share common basic electrophysiological properties (Cepeda *et al.* 2008), we could not identify SONs according to their targets.

Tonic $GABA_A$R-mediated inhibition is weak or absent until the end of the second postnatal week

Spontaneous postsynaptic currents (sPSCs) were observed in all cells examined. When the glutamate receptor antagonists APV (50 μM) and DNQX (10 μM) were present in the superfusion medium, sPSCs were completely and reversibly blocked by either of the selective $GABA_A$ receptor ($GABA_A$R) antagonists bicuculline methiodide (BMI, 20 μM, Fig. 2*A* and *E*) or gabazine (10 μM, data not shown). In the following $GABA_A$-receptor

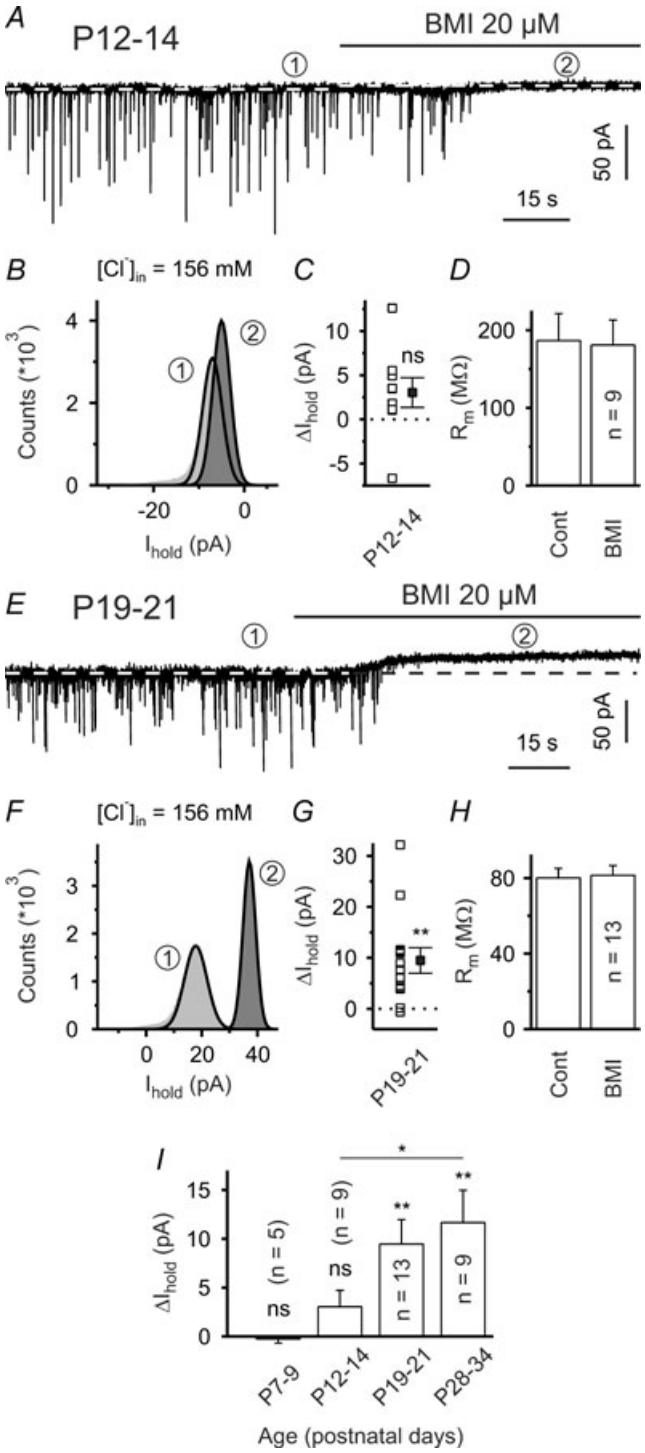

Figure 2. Presence of $GABA_A$R-mediated tonic inward conductance at P19–34, but not P7–14
A, sample trace to illustrate that at P12–14 the mean holding current (indicated by white dashed lines) was only marginally affected by bicuculline methiodide (BMI, 20 μM). Also note that in the presence of ionotropic glutamate receptor antagonists sIPSCs were completely blocked by BMI. In all voltage-clamp experiments the holding potential was set to –70 mV. *B*, all-point histograms constructed from representative 10 s periods in the absence and in the presence of BMI (as indicated by encircled numbers). Thick lines represent Gaussian fits. *C*, quantification of results. Note that in this set of experiments the high Cl^- intrapipette solution was used. *D*, membrane resistance was not affected by BMI. *E*, sample trace to illustrate that at P19–21 application of BMI produced distinct tonic outward currents. *F*, all-point histograms constructed from representative 10 s periods in the absence and in the presence of BMI (as indicated by encircled numbers). Thick lines represent Gaussian fits. *G*, quantification of results. *H*, lack of changes in membrane resistance. *I*, up-regulation of tonic $GABA_A$R-mediated inward conductance during striatal development. Quantification of results. ns – not significant, $^*P < 0.05$, $^{**}P < 0.01$.

mediated PSCs will be referred to as IPSCs although both excitatory and inhibitory GABA actions were found in SONs (Misgeld *et al.* 1982; Bracci & Panzeri, 2006).

A recent report by Ade *et al.* (2008) provided solid evidence for the presence of tonic $GABA_A$R-mediated conductances in SONs. At P12–14, however, we merely detected a non-significant tendency of the mean holding current (I_{hold}) to increase upon BMI (20 μM) application ($\Delta I_{hold} = +3.0 \pm 1.7$ pA, $P = 0.11$, $n = 9$, one-population Student's *t* test; Fig. 2*A*–*C*). Consistently, the membrane resistance was not significantly affected by BMI (186.7 ± 34.8 MΩ in control and 180.9 ± 32.3 MΩ in the presence of BMI, $P > 0.2$, $n = 9$; Fig. 2*D*). In order to facilitate the detection of small currents, a high Cl^- intrapipette solution was used in this set of experiments (see Methods). This result argues against a considerable tonic $GABA_A$R-mediated current. Since this apparent discrepancy with Ade *et al.* (2008) could be due to a difference in age (P12–14 mice *versus* P16–25 mice in the study by Ade *et al.*) we repeated these experiments in slices from older animals (P19–21). In individual cells the BMI-sensitive current displayed considerable variability (ranging from –0.6 pA to +32.2 pA, $n = 13$; Fig. 2*G*). On average, BMI induced a moderate, but significant, outward current (+9.5 ± 2.5 pA, $P < 0.01$, $n = 13$, one-population Student's *t* test; Fig. 2*E*–*G*), but there was no concomitant change in the membrane resistance (80.1 ± 5.1 MΩ in control and 81.5 ± 5.2 MΩ in the presence of BMI, $P > 0.5$, $n = 13$; Fig. 2*H* – these membrane resistance values being similar to those previously reported for this age; Cepeda *et al.* 2004). While BMI did not significantly change I_{hold} at P7–9 (–0.3 ± 0.4 pA, $P > 0.5$, $n = 5$, one-population Student's *t* test; Fig. 2*I*), the BMI-sensitive ΔI_{hold} at P28–34 was similar in magnitude to that of P19–21 mice (+11.7 ± 3.3 pA, $P < 0.01$, $n = 9$, one-population Student's *t* test; Fig. 2*I*). The lack of any detectable effect on the membrane resistance at P19–21 and P28–34 can best be explained by the small total conductance change associated with this tonic current ($G_{tonic}/G_{membrane} \approx 1\%$, i.e. smaller than the typical variance of the membrane resistance during a given condition). Again, it should be emphasized that in all experiments ionotropic glutamate receptor

antagonists were present in the superfusion medium which *per se* might reduce the tonic $GABA_A$R-mediated current in SONs (Ade *et al.* 2008).

We conclude that tonic $GABA_A$R-mediated conductances in SONs are up-regulated during striatal development.

Functional $GABA_B$ receptors are located presynaptically

To examine whether $GABA_B$ receptors ($GABA_B$Rs) influence network activity in P12–14 slices, we applied baclofen, a specific $GABA_B$R agonist. Baclofen (10 μM) drastically decreased the frequency of spontaneous IPSCs from 0.26 ± 0.07 Hz in control to 0.05 ± 0.02 Hz ($P < 0.01$, $n = 6$; Fig. 3*A* and *B*). If $GABA_B$Rs influenced postsynaptic sites (e.g. by activating a K^+ conductance), one could expect a change in membrane resistance and/or holding current upon baclofen application. However, in line with previous reports based on intracellular recording techniques, neither was observed. The mean values for the membrane resistance were 146.5 ± 16.3 MΩ in control and 146.1 ± 16.0 MΩ in the presence of baclofen ($P > 0.9$, $n = 18$; in 12 out of 18 cells QX-314 was present in the pipette). The average change in the mean holding current amounted to -0.9 ± 1.75 pA ($P > 0.5$, one-population Student's *t* test). These results therefore confirm previous electrophysiological as well as immunohistochemical data indicating that SONs do not express functional $GABA_B$Rs (Seabrook *et al.* 1991; Calabresi *et al.* 1991; Nisenbaum *et al.* 1992; Radnikow *et al.* 1997; Ng & Yung, 2001).

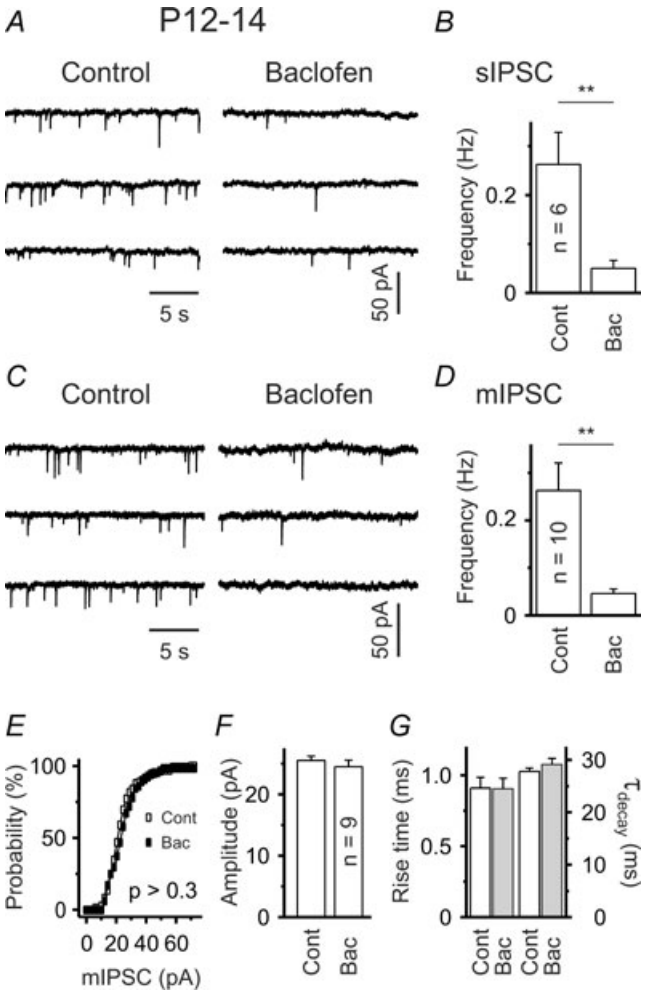

Figure 3. Functional presynaptic $GABA_B$Rs
A and *C*, sample traces show lower sIPSC (*A*) and mIPSC (*C*) frequency in the presence of baclofen (10 μM). *B* and *D*, quantification of results. *E*, mIPSC amplitude distribution is not significantly affected by baclofen (control: open squares, baclofen: filled squares; $P > 0.3$, Kolmogorov–Smirnov test). Plot represents data from a single SON. *F*–*G*, lack of baclofen effect on median mIPSC amplitude, rise time (20–80%) and time constant of decay (mono-exponential fit). $^{**}P < 0.01$.

To corroborate this finding, we next recorded miniature IPSCs (mIPSCs) in the presence of TTX (1 μM), a specific blocker of voltage-gated sodium channels. In order to facilitate quantal analysis, cells with a reasonably high mIPSC frequency under control conditions (i.e. > 0.1 Hz) were selected. It was found that baclofen lacked any significant effect on mIPSC amplitudes (Fig. 3*E* and *F*) and mIPSC kinetics (Fig. 3*G*). The median mIPSC amplitudes were 25.5 ± 0.7 pA and 24.5 ± 1.1 pA ($P > 0.4$, $n = 9$), the mean rise times (20–80%) 0.91 ± 0.08 ms and 0.90 ± 0.05 ms ($P > 0.9$, $n = 9$), and the decay time constants (monoexponential fit) 27.8 ± 0.6 ms and 29.5 ± 1.3 ms ($P > 0.1$, $n = 9$) in control and in the presence of baclofen, respectively. But baclofen consistently reduced the mIPSC frequency from 0.26 ± 0.06 Hz in control to 0.05 ± 0.01 Hz ($P < 0.01$; $n = 10$; Fig. 3*C* and *D*).

We conclude that functional $GABA_B$Rs are located presynaptically and can regulate GABAergic synaptic transmission on SONs.

Presynaptic $GABA_B$Rs are not tonically active under standard conditions

To substantiate our finding, we studied evoked IPSCs (eIPSCs). eIPSCs were elicited via intrastriatal electrical stimulation. In analogy to sIPSCs, eIPSCs were completely and reversibly blocked by BMI (20 μM, $n = 7$, data not shown). At P12–14 baclofen, with a relatively short latency, drastically reduced the amplitude of eIPSCs (Fig. 4*A* and *B*). The mean eIPSC amplitudes were 97.6 ± 21.2 pA and 24.5 ± 5.6 pA in control and in the presence of baclofen, respectively ($P < 0.01$, $n = 12$; Fig. 4*C*). The subsequent application of CGP55845, a specific $GABA_B$R blocker, restored the eIPSC amplitudes to control levels ($P > 0.5$, $n = 12$; Fig. 4*A*–*C*). We obtained equivalent results when using an intrapipette $[Cl^-]$ of 10 mM and

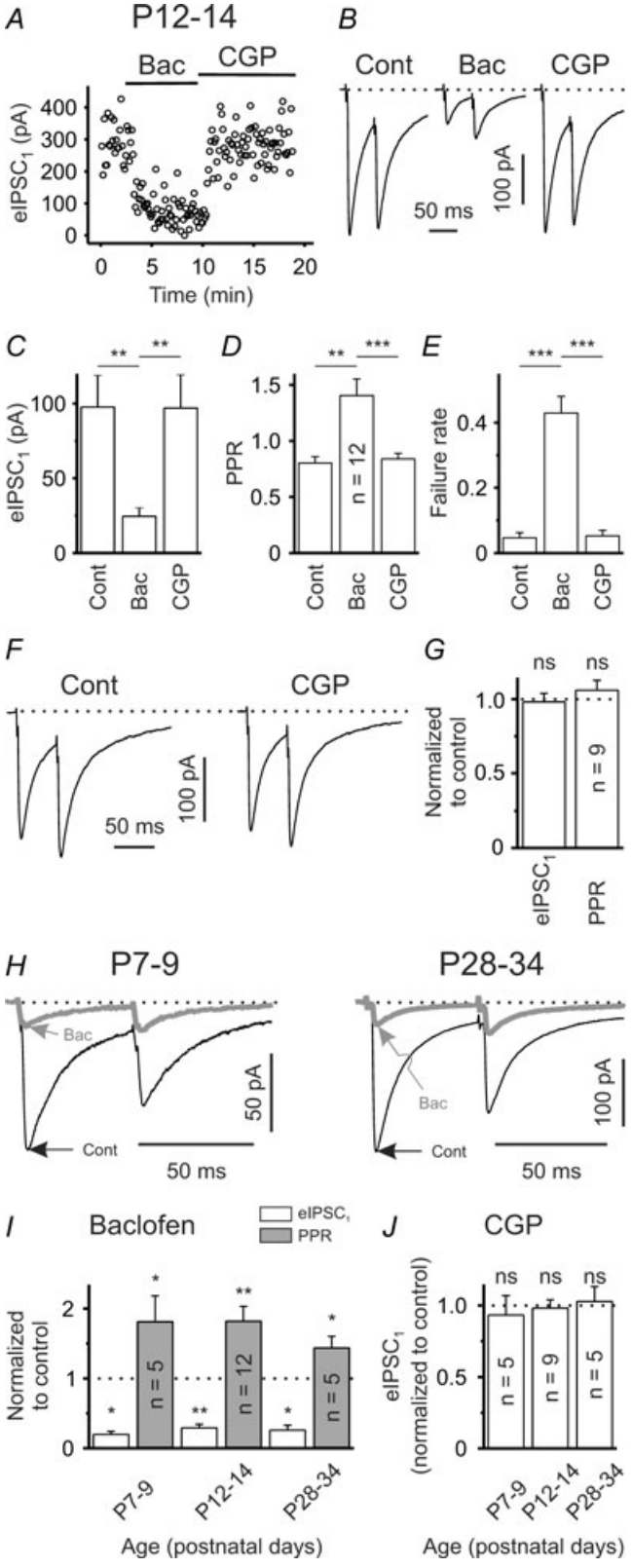

Figure 4. GABA$_B$Rs can constrain the strength of GABAergic synaptic input, but display no tonic activity at rest
A, single experiment to illustrate eIPSC sensitivity to the GABA$_B$R agonist baclofen (10 μM) and the GABA$_B$R antagonist CGP55845 (1 μM) at P12–14. Note relatively short delay between start of application and eIPSC amplitude changes. *B*, eIPSCs in response to paired-pulse stimulation (ISI 50 ms) in control solution and in the presence of either baclofen or CGP55845. Traces represent averages of 20 responses. *C–E*, mean eIPSC$_1$ amplitudes (*C*), PPRs (*D*) and failure rates (*E*) in control solution and in the presence of either baclofen or CGP55845 (all $n = 12$). *F*, eIPSCs in response to paired-pulse stimulation (ISI 50 ms) in control solution and in the presence of CGP55845 without prior application of baclofen. Traces represent averages of 20 responses. *G*, lack of CGP55845 effect on mean eIPSC$_1$ amplitudes and PPRs. *H*, sample traces to illustrate functionality of GABA$_B$R signalling at P7–9 and P28–34. Traces represent averages of 20 responses. *I*, quantification of baclofen effects on eIPSC$_1$ amplitudes and PPRs. *J*, lack of CGP55845 effect on mean eIPSC$_1$ amplitudes at all ages examined (without prior application of baclofen). ns – not significant, $^*P < 0.05$, $^{**}P < 0.01$, $^{***}P < 0.001$.

recording eIPSCs at a holding potential of 0 mV ($n = 3$, see supplemental figure S1A). Under control conditions paired-pulse depression was observed in the majority of cases. Baclofen significantly increased the paired-pulse ratio (PPR, ISI 50 ms) from 0.80 ± 0.06 to 1.41 ± 0.15 ($P < 0.01$, $n = 12$; Fig. 4*B* and *D*). Furthermore, this was associated with an increase in the mean failure rate from 0.05 ± 0.02 to 0.43 ± 0.05 ($P < 0.001$, $n = 12$; Fig. 4*E*). Importantly, the subsequent application of CGP55845 restored both the PPR and the failure rate to control levels ($P > 0.2$ for each parameter, $n = 12$, Fig. 4*B*, *D* and *E*). Although these data strongly argue against a tonic activity of GABA$_B$Rs under control conditions at this age (P12–14), incomplete washout of baclofen could perturb the results. In an attempt to exclude this possibility (in a separate set of experiments) we tested for CGP55845 effects without prior application of baclofen. Similar to the results presented above, CGP55845 did not significantly influence the mean eIPSC amplitude or the PPR ($P > 0.4$ for both parameters, $n = 9$; Fig. 4*F* and *G*).

We next assessed whether GABA$_B$R signalling is functional during earlier and later stages of striatal development. At both P7–9 and P28–34 most of the connections tested displayed paired-pulse depression under control conditions (ISI 50 ms). Baclofen uniformly reduced the amplitude of eIPSCs in both age groups (P7–9: to $19.8 \pm 4.5\%$ of the control value, $P < 0.05$, $n = 5$; P28–34: to $29.1 \pm 5.2\%$ of the control value, $P < 0.05$, $n = 5$; Fig. 4*H* and *I*). Again, this was accompanied by a significant increase of the PPR (P7–9: to $181.2 \pm 37.0\%$ of the control value, $P < 0.05$, $n = 5$; P28–34: to $143.8 \pm 16.3\%$ of the control value, $P < 0.05$, $n = 5$; Fig. 4*H* and *I*). In addition, CGP55845 failed to significantly affect eIPSC amplitudes at both P7–9 and P28–34 (for both age groups $P > 0.4$, $n = 5$; Fig. 4*J*).

We conclude that at all ages examined GABA$_B$Rs (1) can constrain the strength of GABAergic synaptic transmission, but (2) are not tonically active at rest.

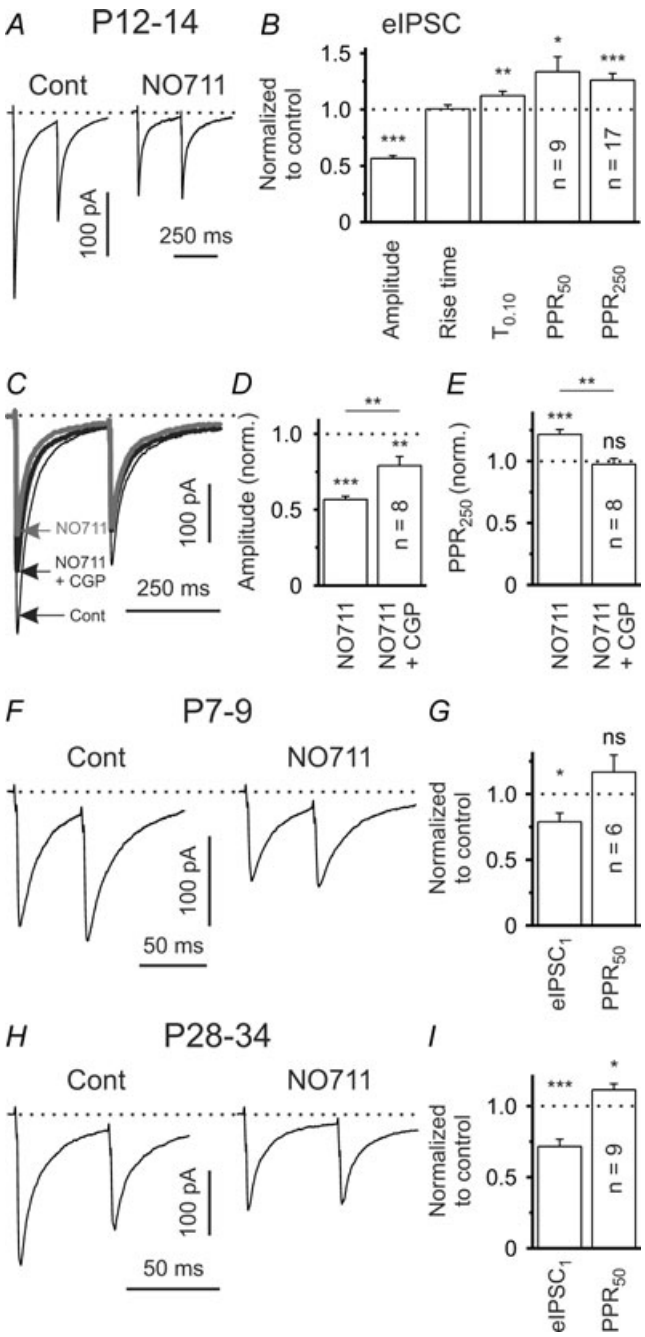

Figure 5. Tonic activation of presynaptic $GABA_BRs$ (P12–34) when activity of GAT-1 is blocked
A, eIPSCs in response to paired-pulse stimulation (ISI 250 ms) in control solution and in the presence of NO-711 (10 μM) at P12–14. Traces represent averages of 20 responses. *B*, quantification of results for NO-711 effects on mean eIPSC amplitude, PPR (PPR_{50}: ISI 50 ms, PPR_{250}: ISI 250 ms), eIPSC rise time (20–80%) and decay ($T_{0.10}$) at P12–14. Data from 17 SONs, except PPR_{50}. *C*, eIPSCs in response to paired-pulse stimulation (ISI 250 ms) in control solution and in the presence of either NO-711 or NO-711 plus CGP55845 (1 μM). Traces represent averages of 20 responses. *D–E*, CGP55845 partially restored the NO-711-induced reduction in eIPSC amplitude and completely reversed the NO-711-induced increase in PPR (ISI 250 ms). *F*, eIPSCs in response to paired-pulse stimulation in control solution and in the presence of NO-711 at P7–9. Traces represent averages of 20 responses. *G*, quantification of results for NO-711 effects on eIPSC amplitude and PPR at P7–9. *H*, eIPSCs in response to paired-pulse stimulation in control solution and in the presence of NO-711 at P28–34. Traces represent averages of 20 responses. *I*, Quantification of results for NO-711 effects on eIPSC amplitude and PPR at P28–34. ns – not significant, $^*P < 0.05$, $^{**}P < 0.01$, $^{***}P < 0.001$.

GAT-1 activity precludes tonic activation of $GABA_BRs$ under resting conditions

Previous anatomical studies indicated that GAT-1 is the predominant GAT subtype in the adult rodent neostriatum (e.g. Ikegaki *et al.* 1994; Durkin *et al.* 1995). The lack of a distinct tonic $GABA_AR$ and $GABA_BR$ activation under standard conditions at P12–14 suggests that GABA clearance of the extracellular space by GATs is relatively efficient. But do GATs shape GABAergic synaptic transmission on SONs at this age? To address this important question we applied NO-711, a specific blocker of GAT-1, and recorded eIPSCs. NO-711 (10 μM) significantly decreased the amplitude of eIPSCs to $56.6 \pm 2.4\%$ of the control value ($P < 0.001$, $n = 17$, one-population Student's t test; Fig. 5*A* and *B*). Again, similar results were obtained with a close to physiological $[Cl^-]_i$ at a holding potential of 0 mV ($n = 3$, see supplemental figure S1B). We next examined the decay of eIPSCs and measured the time taken for the current to decay to 10% of the peak amplitude ($T_{0.10}$). NO-711 slightly, but significantly, prolonged $T_{0.10}$ from 145.5 ± 8.5 ms in control to 164.1 ± 11.6 ms ($P < 0.01$, $n = 17$; Fig. 5*B*) suggesting that GAT-1 operates in the uptake mode and assists the clearance of GABA from the synaptic cleft (see, for instance Thompson & Gahwiler, 1992; Overstreet & Westbrook, 2003; Kirmse & Kirischuk, 2006). If GAT-1 were operating in the uptake mode, its block would be expected to result in an increase of extracellular GABA concentration and this might lead to activation of presynaptic $GABA_BRs$. Indeed, the lower eIPSC amplitudes in the presence of NO-711 were associated with a significant increase of the PPR to $133.5 \pm 13.2\%$ ($P < 0.05$, $n = 9$, one-population Student's t test; Fig. 5*B*, PPR_{50}) and $126.1 \pm 5.8\%$ ($P < 0.001$, $n = 17$, one-population Student's t test; Fig. 5*B*, PPR_{250}) of control for ISIs of 50 ms and 250 ms, respectively. Coapplication of CGP55845 in the presence of NO-711 only partly restored the eIPSC amplitude ($79.1 \pm 5.9\%$ of the control value, $P < 0.01$, $n = 8$, one-population Student's t test; Fig. 5*C* and *D*), but reduced the PPR to control levels ($97.5 \pm 4.8\%$ of the control value, $P > 0.6$, $n = 8$, one-population Student's t test; Fig. 5*C* and *E*). Taken together, these data indicate that, at P12–14, NO-711 reduces eIPSC amplitudes due to $GABA_BR$-dependent and $GABA_BR$-independent mechanisms.

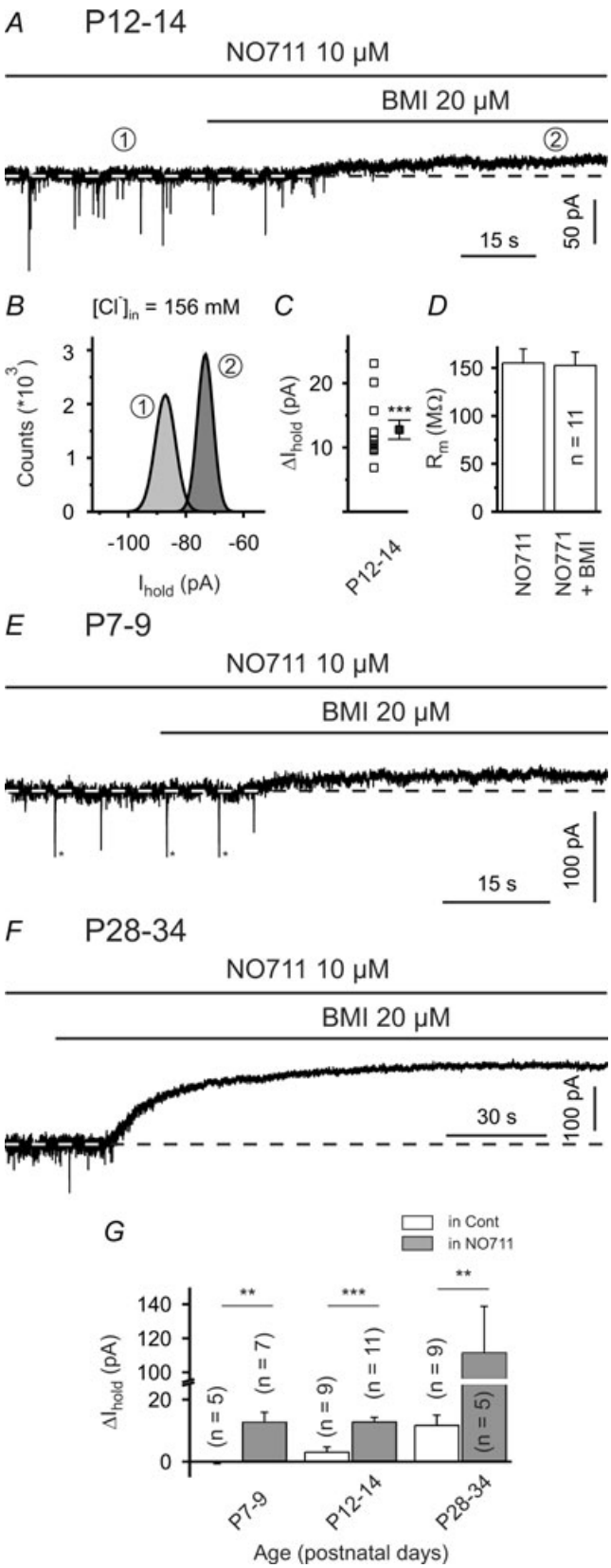

We next assessed whether GAT-1 is functional at an earlier stage of striatal development (P7–9). It turned out that NO-711 significantly reduced the eIPSC amplitudes to 78.9 ± 6.6% of the control value ($P < 0.05$, $n = 6$; Fig. 5*F* and *G*). However, this effect was not accompanied by a significant change of the PPR_{50} (116.7 ± 12.9% of the control value, $P > 0.2$, $n = 6$; Fig. 5*F* and *G*). Accordingly, coapplication of CGP55845 in the presence of NO-711 did not increase the eIPSC amplitudes (93.6 ± 8.6% – normalized to values obtained in the presence of NO-711, $P > 0.25$, $n = 6$). This argues against a distinct $GABA_BR$ activation during GAT-1 block at P7–9.

The results obtained from P28–34 mice were very similar to those from P12–14 mice, i.e. NO-711 reduced eIPSC amplitudes (to 71.6 ± 5.1% of the control value, $P < 0.001$, $n = 9$; one-population Student's *t* test; Fig. 5*H* and *I*) and increased the PPR_{50} (to 111.4 ± 4.3% of the control value, $P < 0.05$, $n = 9$; one-population Student's *t* test; Fig. 5*H* and *I*). Coapplication of CGP55845 in the presence of NO-711 partly restored the eIPSC amplitudes ($P < 0.05$, $n = 5$; data not shown) indicating a persistent activation of $GABA_BRs$ during GAT-1 block at an almost mature stage.

GAT-1 limits the tonic activation of postsynaptic $GABA_ARs$

As shown before, a $GABA_BR$-independent mechanism contributed to the observed decrease in eIPSC amplitudes at all ages examined. A possible explanation for this observation could be postsynaptic shunting due to a persistent activation of ionotropic $GABA_ARs$ by a higher ambient GABA concentration in the presence of NO-711, i.e. tonic inhibition.

However, at P12–14 NO-711 failed to alter the membrane resistance of SONs (176.7 ± 24.4 MΩ in control and 172.1 ± 21.1 MΩ in the presence of NO-711, $P > 0.4$, $n = 17$) at low intrapipette Cl^- concentration. We also examined whether GAT-1

Figure 6. Block of GAT-1 facilitates tonic activation of postsynaptic $GABA_ARs$
A, sample trace showing that, at P12–14, BMI (20 µM) induced a distinct outward current in the presence of NO-711 (and ionotropic glutamate receptor antagonists). In all voltage-clamp experiments the holding potential was set to –70 mV. *B*, all-point histograms constructed from representative 10 s periods in the absence and presence of BMI (as indicated by encircled numbers). Thick lines represent Gaussian fits. *C* and *D*, quantification of results for BMI effects in the presence of NO-711 at P12–14. Note use of high Cl^- intrapipette solution. *E* and *F*, sample traces showing that BMI (20 µM) induced a distinct outward current in the presence of NO-711 at both P7–9 (*E*) and P28–34 (*F*; note scaling). Asterisks (*) in *E* indicate clipping. *G*, quantification of results for BMI effects in control solution (hollow bars) and in the presence of NO-711 (grey bars). Note axis break of the ordinate. ns – not significant, $^{**}P < 0.01$, $^{***}P < 0.001$.

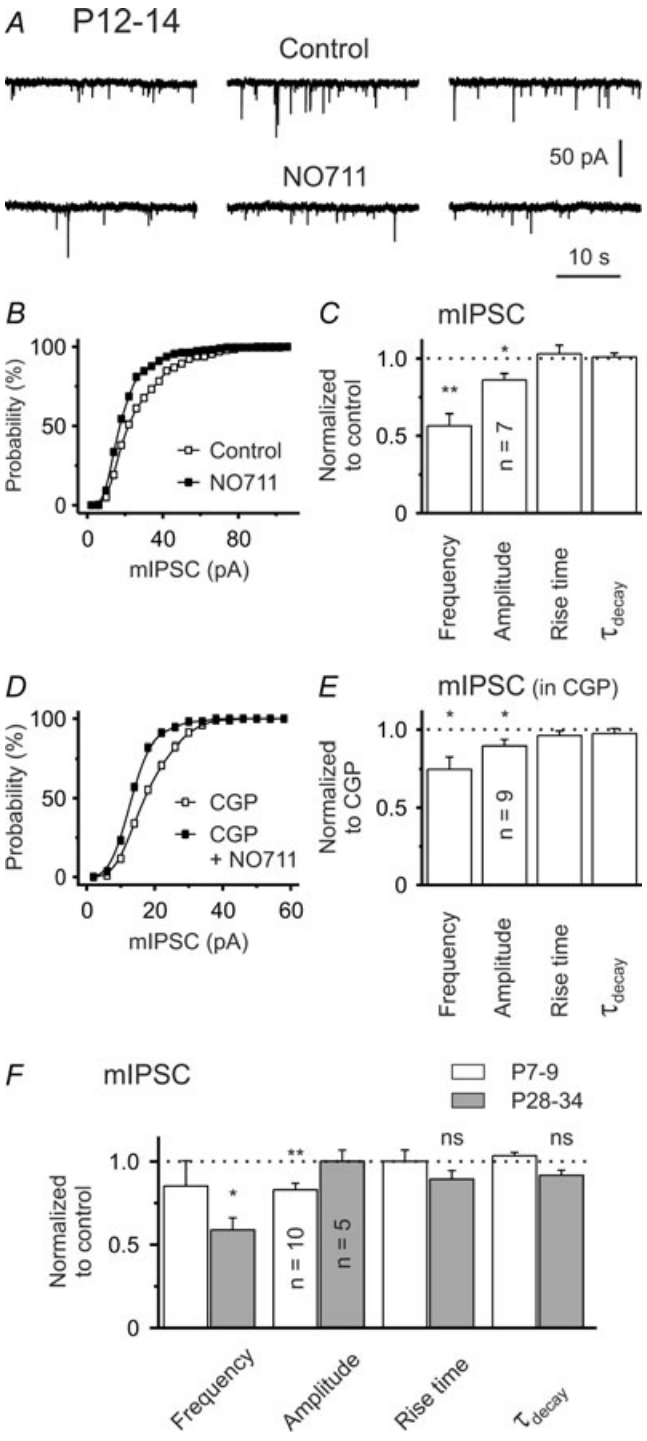

Figure 7. GAT-1 block reduces the median amplitude of mIPSCs
A, sample traces at P12–14. *B*, NO-711 shifted the mIPSC amplitude distribution to the left. Data from same cell as in *A*. *C*, quantification of results for NO-711 effects. *D*, leftward shift of mIPSC amplitude distribution by NO-711 in the presence of CGP55845.
E, quantification of results for NO-711 in the presence of CGP55845. *F*, summary of NO711 effects on mIPSCs at P7–9 and P28–34. ns – not significant, $^{*}P < 0.05$, $^{**}P < 0.01$.

block could produce a BMI-sensitive change in the holding current (ΔI_{hold}). Again, we used a high Cl^- intrapipette solution to increase the driving force for Cl^- flow. It turned out that BMI (20 μM) reliably induced an outward current of 12.8 ± 1.5 pA ($P < 0.001$, $n = 11$, one-population Student's t test; Fig. 6*A–C*; calculated $G_{tonic}/G_{membrane} \approx 2.5\%$). ΔI_{hold} was significantly higher than that in the absence of NO-711 ($P < 0.001$, unpaired Student's t test; cf. Fig. 6*G*). However, ΔI_{hold} was not accompanied by a significant change in the membrane resistance (155.2 ± 14.8 MΩ and 152.6 ± 14.0 MΩ in the presence of NO-711 and NO-711 plus BMI, respectively, $P > 0.1$, $n = 11$; Fig. 6*D*).

Whereas no tonic $GABA_A$R-mediated current was seen under control conditions at P7–9, BMI did induce a distinct ΔI_{hold} when applied in the presence of NO-711 (12.7 ± 3.2 pA, $P < 0.01$, $n = 7$, Fig. 6*E* and *G*). At P28–34 tonic activation of $GABA_A$Rs has already been observed under standard conditions (Fig. 2*I*). However, BMI induced a more pronounced tonic outward current when GAT-1 was blocked (mean $\Delta I_{hold} = 111.4 \pm 27.4$ pA, $P < 0.01$, $n = 5$; Fig. 6*F* and *G*). Moreover, in this case the BMI-induced ΔI_{hold} was accompanied by a significant increase in the membrane resistance to $114.5 \pm 3.0\%$ of the control value ($P < 0.05$, $n = 5$).

At P28–34 we observed a moderate correlation between the NO-711-induced relative reduction of the mean eIPSC amplitude and ΔI_{hold} ($R^2 = 0.46$, $P = 0.044$, $n = 9$ cells, data not shown). This indicates that postsynaptic shunting might add to the reduction of eIPSC amplitudes at this age. However, whereas we detected marked differences in ΔI_{hold} between the age groups (cf. Fig. 6*G*), the $GABA_B$R-independent reduction of eIPSC amplitudes was rather similar (~25%, cf. Fig. 5*B–D*, *G* and *I*). We therefore favour the idea that a further, $GABA_B$R- and shunting-independent, factor contributes to the observed NO-711-induced eIPSC suppression.

GAT-1 ensures stability of the quantal amplitudes

To further analyse the nature of the $GABA_B$R-independent component of the eIPSC decrease during GAT-1 block, we recorded mIPSCs. It turned out that, at P12–14, NO-711 strongly decreased the frequency of mIPSCs to $56 \pm 8\%$ of the control value ($P < 0.01$, $n = 7$, one-population Student's t test; Fig. 7*A* and *C*), without affecting the mIPSC kinetics (Fig. 7*C*). This supports our suggestion that GAT-1 operates in the uptake mode and its block results in an activation of presynaptic $GABA_B$Rs. Concomitantly, NO-711 significantly reduced the median mIPSC amplitude to $86 \pm 4\%$ ($P < 0.05$, $n = 7$, one-population Student's t test, Fig. 7*A–C*). As expected, a comparable reduction of median mIPSC amplitudes was observed when NO-711 was applied in the presence

of CGP55845 ($P < 0.05$, $n = 9$, one-population Student's t test; Fig. 7D and E) indicating that it is independent of $GABA_BR$ activation. Interestingly, even in the presence of CGP55845, a significant, albeit less pronounced, reduction in mIPSC frequency was noted ($P < 0.05$, $n = 9$, one-population Student's t test; Fig. 7E). The latter result suggests that reduced detection of small mIPSCs could contribute to the observed decrease in mIPSC frequency.

At P7–9 NO-711 led to a similar reduction of the median mIPSC amplitude ($83.0 \pm 3.9\%$ of the control value, $P < 0.01$, $n = 10$, one-population Student's t test; Fig. 7F), without significantly affecting mIPSC kinetics (Fig. 7F). The decrease in mIPSC frequency was non-significant, supporting our notion that $GABA_BR$ activation during GAT-1 block is weak or absent at this age.

At P28–34 NO-711 lacked any significant effect on mIPSC amplitudes ($P > 0.8$, $n = 5$, Fig. 7F) and kinetics ($P = 0.08$, $n = 5$, Fig. 7F), but markedly reduced mIPSC frequency to $58.9 \pm 7.2\%$ of the control value ($P < 0.05$, $n = 5$, Fig. 7F). However, the analysis of mIPSCs at this age was complicated by the fact that NO-711 produced not only large baseline shifts (even in the presence of TTX), but also a considerable increase in baseline noise. Accordingly, a lack of NO-711 effects on median mIPSC amplitudes at this age might well represent a false-negative result, as small mIPSCs are expected to escape detection under these circumstances. Therefore, we favour the idea that a reduction of the quantal amplitude (as detected at the soma) contributes to the observed $GABA_BR$-independent component of the eIPSC amplitude decrease during GAT-1 block.

Discussion

The present experiments revealed a significant influence of GABA transporter 1 on GABAergic synaptic transmission at putative striatal output neurons (SONs) in the juvenile and quasi-mature rodent neostriatum. Based on the obtained electrophysiological data we report that: (1) GAT-1 is functional throughout striatal development (P7–34) and operates in a net uptake mode, (2) GAT-1 shortens the duration of the postsynaptic response, (3) presynaptically located $GABA_BRs$ can constrain the strength of GABAergic synapses on SONs at all ages examined, but they are not tonically active under resting conditions, (4) GAT-1 determines the activity of presynaptic $GABA_BRs$ (P12–34) and limits the activation of postsynaptic $GABA_ARs$ (P7–34), and (5) GAT-1 activity is necessary for maintaining the quantal size. The cartoon of supplemental figure S2 illustrates these results.

$GABA_BR$-mediated inhibition of GABA release

$GABA_BR$-mediated inhibition of synaptic GABA release on striatal neurons of adult rats has been documented by several groups using intracellular recording techniques (Seabrook *et al.* 1991; Calabresi *et al.* 1991; Nisenbaum *et al.* 1992; Radnikow *et al.* 1997). In the present study we revealed that $GABA_BR$ signalling is operative even at early stages of striatal development (as early as P7–9). In line with the above-mentioned studies, we were not able to detect any postsynaptic effect of $GABA_BR$ modulators on SONs in the juvenile striatum. Accordingly, baclofen did not induce a tonic current or change in membrane resistance, and it did not affect mIPSC amplitude or kinetics. In contrast to data obtained in striatal culture (Behrends & Ten Bruggencate, 1998), the latter result further suggests that the quantal size (as reflected in the median mIPSC amplitude) is independent of GABA release probability in our preparation. The lack of postsynaptic effects reported here is supported by recent immunohistochemical data indicating the absence of (somatic) $GABA_BR2$ subunits in SONs (Ng & Yung, 2001). On the other hand, using pre-embedding immunogold electron microscopy Lacey *et al.* (2005) have shown that $GABA_BR1$ and $GABA_BR2$ subunits (both of which are required for heterodimerization into functional $GABA_BRs$; Kaupmann *et al.* 1998) are expressed at both presynaptic and postsynaptic sites of symmetrical, putative GABAergic contacts. However, most of the labelling in the postsynaptic cells was observed in the cytosol suggesting that few, if any, functional $GABA_BRs$ exist in the somato-dendritic membrane.

Activation of $GABA_BRs$ with baclofen reduced the amplitudes of eIPSCs in all cells and at all ages tested. With respect to $GABA_BR$ sensitivity, our data do not support the existence of two populations of GABAergic inputs as it was suggested by previous studies (adult rats: Seabrook *et al.* 1991; Radnikow *et al.* 1997). This discrepancy might be derived from the methods used (lower resolution with conventional intracellular recording techniques) and/or differences in age. It should be noted that somatic recordings are expected to primarily reflect GABAergic afferents synapsing on the soma or proximal dendrites of SONs (as is typical of fast-spiking interneuron collaterals; see also below). Accordingly, we cannot exclude that more distally located GABAergic synapses (e.g. synapses formed by axon collaterals of SONs themselves) were underrepresented here and differed in $GABA_BR$ sensitivity.

Tonic activation of $GABA_ARs$ in SONs

In contrast to a previous study of the adult rat striatum (Calabresi *et al.* 1991), our present data revealed no evidence for tonic activation of presynaptic $GABA_BRs$, which suggests that ambient GABA concentration is low in our preparation. Likewise, we were unable to detect a tonic $GABA_AR$-mediated current until the end of the second postnatal week (P7–9 and P12–14). In contrast, at

older ages (P19–21 and P28–34) a BMI-sensitive tonic current was clearly present, thereby supporting a previous observation by Ade *et al.* (2008) in P16–25 mice. Interestingly, this period of age covers the time of most active synaptogenesis in the cortico-striatal synapse pathway (Tepper *et al.* 1998; Uryu *et al.* 1999). Therefore, it is tempting to speculate that an increase in synaptic GABA release, due to an up-regulation of the glutamatergic 'drive' of GABAergic SONs and interneurons, could account for the persistent activation of postsynaptic $GABA_A$Rs (and possibly presynaptic $GABA_B$Rs) at older ages. Definitely, further investigations are necessary to corroborate this hypothesis.

Extrasynaptic $GABA_A$Rs (those that presumably underlie tonic inhibition in SONs) and metabotropic $GABA_B$Rs (at presynaptic terminals of afferents to SONs) are both high-affinity receptors for GABA. It is somewhat surprising that we observed distinct BMI-sensitive tonic currents at P28–34 (suggesting persistent $GABA_A$R activation), but found no compelling evidence for a tonic activation of presynaptic $GABA_B$Rs. This discrepancy might potentially reflect spatial inhomogeneities of extracellular GABA concentration although several other possible explanations exist (e.g. differences in GABA affinities, lower sensitivity to detect $GABA_B$R activation with the method used). In such a scenario GAT-1 might create a specific (low [GABA]) (peri)synaptic environment thereby preventing presynaptic $GABA_B$Rs and postsynaptic $GABA_A$Rs from detecting higher ambient GABA concentrations.

GAT-1 activity shapes GABAergic synaptic transmission on SONs

In general, GAT-1 is abundant in presynaptic GABAergic terminals as well as in distal astrocytic processes (for review see Gadea & Lopez-Colome, 2001). Hence, GAT-1 is in a good position to control GABAergic synaptic transmission. Currently, however, data regarding the precise cellular and subcellular distribution of GAT-1 (protein) are not yet available for the striatum. Using light microscopic autoradiography, Bolam *et al.* (1983) identified a population of medium-sized aspiny cells that selectively took up [^{3}H]GABA after local injection into the neostriatum. These cells exhibited morphological characteristics typical of local circuit neurons. In the neostriatum of adult rats GAT-1 mRNA was only found in a small fraction of cells coexpressing GAD67 (Augood *et al.* 1995). The majority of these cells were immunopositive for parvalbumin, a marker of striatal FS interneurons. Considering the currently observed consistency of NO-711 effects on the GABAergic synaptic transmission, it seems rather likely that our extracellular stimulation mainly targeted axons originating from FS interneurons. Although clearly speculative, this notion is also supported by the fact that FS interneurons (1) mature earlier than SONs (Tepper *et al.* 1998; Plotkin *et al.* 2005) and (2) form stronger (large unitary eIPSC amplitudes) and more reliable (low failure rate of unitary eIPSCs) synaptic connections with SONs (Koos *et al.* 2004, but see Venance *et al.* 2004).

Our data show that GABA uptake via GAT-1 is functional throughout the developmental period studied here. In line with this conclusion, GAT-1 limits tonic $GABA_A$R-mediated conductances in all age groups (P7–34). Furthermore (peri)synaptically located GAT-1 constrains the activation of presynaptic $GABA_B$Rs (at least from P12 onward), mediates the clearance of GABA from the synaptic cleft and ensures stability of the quantal amplitude (as detected at the soma). The latter effect appears to be independent of $GABA_B$R activation, as the reduction of median mIPSC amplitudes by NO-711 persisted in the presence of CGP55845. We did not aim at clarifying the precise mechanism of mIPSC suppression. In principle, it may have a postsynaptic (for instance desensitization of $GABA_A$Rs (Overstreet *et al.* 2000) or shunting) and/or presynaptic (for instance decreased vesicle filling; Zhou *et al.* 2000; Engel *et al.* 2001; Kirmse & Kirischuk, 2006) origin.

Considering that GAT-1 has considerable impact on GABAergic synaptic transmission in SONs, the identification of stimuli that control the activity/expression of this transporter and its reversal potential is expected to add a further level of regulatory complexity. In this context, it is relevant that glutamate- and dopamine-evoked non-vesicular, transporter-mediated [^{3}H]GABA efflux from rat striatal cultures has been reported in previous pharmacological studies (Weiss, 1988; Schoffelmeer *et al.* 2000). An elevation of intracellular [Na^+], as a result of Na^+ entry through NMDA receptor channels and protein kinase A-dependent inhibition of Na^+/K^+-ATPase activity, has been suggested to reverse the operation of the GABA transporter and, consequently, to produce higher extracellular GABA concentrations (Schoffelmeer *et al.* 2000). Therefore, $GABA_B$R-mediated inhibition could theoretically become operative even in the absence of surplus synaptic release of GABA. Similar considerations might apply to glutamatergic cortico-striatal synapses that are also subject to regulation by presynaptic $GABA_B$Rs (Calabresi *et al.* 1991 and autors' unpublished observations).

Concluding remarks

We provide, for the first time, direct physiological evidence for a role of GABA transporter 1 in the regulation of GABAergic synaptic transmission in the murine

neostriatum. These results might be of importance for the understanding of certain pathological states, where intrastriatal GABAergic signalling is disease-relevant (e.g. Parkinson's disease (Mallet *et al.* 2006), Huntington's disease (Cepeda *et al.* 2004) and substance abuse (Del Arco *et al.* 1998)). A major open question to be answered by further experiments is to what extent tonic GAT-dependent depolarizing actions of GABA in the juvenile or adult striatum may contribute to pathological states associated with neuron loss.

References

Ade KK, Janssen MJ, Ortinski PI & Vicini S (2008). Differential tonic GABA conductances in striatal medium spiny neurons. *J Neurosci* **28**, 1185–1197.

Augood SJ, Herbison AE & Emson PC (1995). Localization of GAT-1 GABA transporter mRNA in rat striatum: cellular coexpression with GAD67 mRNA, GAD67 immunoreactivity, and parvalbumin mRNA. *J Neurosci* **15**, 865–874.

Balleine BW, Delgado MR & Hikosaka O (2007). The role of the dorsal striatum in reward and decision-making. *J Neurosci* **27**, 8161–8165.

Behrends JC & ten Bruggencate G (1998). Changes in quantal size distributions upon experimental variations in the probability of release at striatal inhibitory synapses. *J Neurophysiol* **79**, 2999–3011.

Bolam JP, Clarke DJ, Smith AD & Somogyi P (1983). A type of aspiny neuron in the rat neostriatum accumulates [^{3}H]γ-aminobutyric acid: combination of Golgi-staining, autoradiography, and electron microscopy. *J Comp Neurol* **213**, 121–134.

Bracci E & Panzeri S (2006). Excitatory GABAergic effects in striatal projection neurons. *J Neurophysiol* **95**, 1285–1290.

Calabresi P, Mercuri NB, De Murtas M & Bernardi G (1991). Involvement of GABA systems in feedback regulation of glutamate-and GABA-mediated synaptic potentials in rat neostriatum. *J Physiol* **440**, 581–599.

Cavelier P, Hamann M, Rossi D, Mobbs P & Attwell D (2005). Tonic excitation and inhibition of neurons: ambient transmitter sources and computational consequences. *Prog Biophys Mol Biol* **87**, 3–16.

Cepeda C, Andre VM, Yamazaki I, Wu N, Kleiman-Weiner M & Levine MS (2008). Differential electrophysiological properties of dopamine D1 and D2 receptor-containing striatal medium-sized spiny neurons. *Eur J Neurosci* **27**, 671–682.

Cepeda C, Starling AJ, Wu N, Nguyen OK, Uzgil B, Soda T, Andre VM, Ariano MA & Levine MS (2004). Increased GABAergic function in mouse models of Huntington's disease: reversal by BDNF. *J Neurosci Res* **78**, 855–867.

Chronister RB, Farnell KE, Marco LA & White LE Jr (1976). The rodent neostriatum: a Golgi analysis. *Brain Res* **108**, 37–46.

Del Arco A, Castaneda TR & Mora F (1998). Amphetamine releases GABA in striatum of the freely moving rat: involvement of calcium and high affinity transporter mechanisms. *Neuropharmacology* **37**, 199–205.

Durkin MM, Smith KE, Borden LA, Weinshank RL, Branchek TA & Gustafson EL (1995). Localization of messenger RNAs encoding three GABA transporters in rat brain: an in situ hybridization study. *Brain Res Mol Brain Res* **33**, 7–21.

Engel D, Pahner I, Schulze K, Frahm C, Jarry H, Ahnert-Hilger G & Draguhn A (2001). Plasticity of rat central inhibitory synapses through GABA metabolism. *J Physiol* **535**, 473–482.

Gadea A & Lopez-Colome AM (2001). Glial transporters for glutamate, glycine, and GABA. II. GABA transporters. *J Neurosci Res* **63**, 461–468.

Gerfen CR (1992). The neostriatal mosaic: multiple levels of compartmental organization. *Trends Neurosci* **15**, 133–139.

Glykys J & Mody I (2007). The main source of ambient GABA responsible for tonic inhibition in the mouse hippocampus. *J Physiol* **582**, 1163–1178.

Hattori T & McGeer PL (1973). Synaptogenesis in the corpus striatum of infant rat. *Exp Neurol* **38**, 70–79.

Ikegaki N, Saito N, Hashima M & Tanaka C (1994). Production of specific antibodies against GABA transporter subtypes (GAT1, GAT2, GAT3) and their application to immunocytochemistry. *Brain Res Mol Brain Res* **26**, 47–54.

Ingham CA, Hood SH, Taggart P & Arbuthnott GW (1998). Plasticity of synapses in the rat neostriatum after unilateral lesion of the nigrostriatal dopaminergic pathway. *J Neurosci* **18**, 4732–4743.

Jursky F & Nelson N (1996). Developmental expression of GABA transporters GAT1 and GAT4 suggests involvement in brain maturation. *J Neurochem* **67**, 857–867.

Kaupmann K, Malitschek B, Schuler V, Heid J, Froestl W, Beck P, Mosbacher J, Bischoff S, Kulik A, Shigemoto R, Karschin A & Bettler B (1998). $GABA_B$-receptor subtypes assemble into functional heteromeric complexes. *Nature* **396**, 683–687.

Kawaguchi Y, Wilson CJ, Augood SJ & Emson PC (1995). Striatal interneurones: chemical, physiological and morphological characterization. *Trends Neurosci* **18**, 527–535.

Kirmse K, Dvorzhak A, Henneberger C, Grantyn R & Kirischuk S (2007). Cajal Retzius cells in the mouse neocortex receive two types of pre- and postsynaptically distinct GABAergic inputs. *J Physiol* **585**, 881–895.

Kirmse K & Kirischuk S (2006). Ambient GABA constrains the strength of GABAergic synapses at Cajal-Retzius cells in the developing visual cortex. *J Neurosci* **26**, 4216–4227.

Kita T, Kita H & Kitai ST (1984). Passive electrical membrane properties of rat neostriatal neurons in an in vitro slice preparation. *Brain Res* **300**, 129–139.

Koos T, Tepper JM & Wilson CJ (2004). Comparison of IPSCs evoked by spiny and fast-spiking neurons in the neostriatum. *J Neurosci* **24**, 7916–7922.

Lacey CJ, Boyes J, Gerlach O, Chen L, Magill PJ & Bolam JP (2005). $GABA_B$ receptors at glutamatergic synapses in the rat striatum. *Neuroscience* **136**, 1083–1095.

Mallet N, Ballion B, Le Moine C & Gonon F (2006). Cortical inputs and GABA interneurons imbalance projection neurons in the striatum of parkinsonian rats. *J Neurosci* **26**, 3875–3884.

Misgeld U, Dodt HU & Frotscher M (1986). Late development of intrinsic excitation in the rat neostriatum: an in vitro study. *Brain Res* **392**, 59–67.

Misgeld U, Wagner A & Ohno T (1982). Depolarizing IPSPs and depolarization by GABA of rat neostriatum cells in vitro. *Exp Brain Res* **45**, 108–114.

Ng TK & Yung KK (2001). Differential expression of $GABA_B$ R1 and $GABA_B$R2 receptor immunoreactivity in neurochemically identified neurons of the rat neostriatum. *J Comp Neurol* **433**, 458–470.

Nisenbaum ES & Berger TW (1992). Functionally distinct subpopulations of striatal neurons are differentially regulated by GABAergic and dopaminergic inputs – I. In vivo analysis. *Neuroscience* **48**, 561–578.

Nisenbaum ES, Berger TW & Grace AA (1992). Presynaptic modulation by $GABA_B$ receptors of glutamatergic excitation and GABAergic inhibition of neostriatal neurons. *J Neurophysiol* **67**, 477–481.

Nisenbaum ES & Wilson CJ (1995). Potassium currents responsible for inward and outward rectification in rat neostriatal spiny projection neurons. *J Neurosci* **15**, 4449–4463.

Overstreet LS, Jones MV & Westbrook GL (2000). Slow desensitization regulates the availability of synaptic $GABA_A$ receptors. *J Neurosci* **20**, 7914–7921.

Overstreet LS & Westbrook GL (2003). Synapse density regulates independence at unitary inhibitory synapses. *J Neurosci* **23**, 2618–2626.

Plotkin JL, Wu N, Chesselet MF & Levine MS (2005). Functional and molecular development of striatal fast-spiking GABAergic interneurons and their cortical inputs. *Eur J Neurosci* **22**, 1097–1108.

Radnikow G, Rohrbacher J & Misgeld U (1997). Heterogeneity in use-dependent depression of inhibitory postsynaptic potentials in the rat neostriatum in vitro. *J Neurophysiol* **77**, 427–434.

Richerson GB & Wu Y (2003). Dynamic equilibrium of neurotransmitter transporters: not just for reuptake anymore. *J Neurophysiol* **90**, 1363–1374.

Schoffelmeer AN, Vanderschuren LJ, De Vries TJ, Hogenboom F, Wardeh G & Mulder AH (2000). Synergistically interacting dopamine D1 and NMDA receptors mediate nonvesicular transporter-dependent GABA release from rat striatal medium spiny neurons. *J Neurosci* **20**, 3496–3503.

Seabrook GR, Howson W & Lacey MG (1991). Subpopulations of GABA-mediated synaptic potentials in slices of rat dorsal striatum are differentially modulated by presynaptic $GABA_B$ receptors. *Brain Res* **562**, 332–334.

Tepper JM, Sharpe NA, Koos TZ & Trent F (1998). Postnatal development of the rat neostriatum: electrophysiological, light- and electron-microscopic studies. *Dev Neurosci* **20**, 125–145.

Tepper JM, Wilson CJ & Koos T (2008). Feedforward and feedback inhibition in neostriatal GABAergic spiny neurons. *Brain Res Rev* **58**, 272–281.

Thompson SM & Gahwiler BH (1992). Effects of the GABA uptake inhibitor tiagabine on inhibitory synaptic potentials in rat hippocampal slice cultures. *J Neurophysiol* **67**, 1698–1701.

Tyzio R, Ivanov A, Bernard C, Holmes GL, Ben Ari Y & Khazipov R (2003). Membrane potential of CA3 hippocampal pyramidal cells during postnatal development. *J Neurophysiol* **90**, 2964–2972.

Uryu K, Butler AK & Chesselet MF (1999). Synaptogenesis and ultrastructural localization of the polysialylated neural cell adhesion molecule in the developing striatum. *J Comp Neurol* **405**, 216–232.

Venance L, Glowinski J & Giaume C (2004). Electrical and chemical transmission between striatal GABAergic output neurones in rat brain slices. *J Physiol* **559**, 215–230.

Weiss S (1988). Excitatory amino acid-evoked release of γ-[^{3}H]aminobutyric acid from striatal neurons in primary culture. *J Neurochem* **51**, 435–441.

Yamada H, Fujimoto K & Yoshida M (1995). Neuronal mechanism underlying dystonia induced by bicuculline injection into the putamen of the cat. *Brain Res* **677**, 333–336.

Yoshida M, Nagatsuka Y, Muramatsu S & Niijima K (1991). Differential roles of the caudate nucleus and putamen in motor behavior of the cat as investigated by local injection of GABA antagonists. *Neurosci Res* **10**, 34–51.

Zhou Q, Petersen CC & Nicoll RA (2000). Effects of reduced vesicular filling on synaptic transmission in rat hippocampal neurones. *J Physiol* **525**, 195–206.

Acknowledgements

We thank Donald S. Faber (New York) for helpful comments on earlier versions of the manuscript. The technical assistance of Mrs Kerstin Rückwardt is highly appreciated. This study was supported by the German Research Council (Deutsche Forschungsgemeinschaft, Gr 986/9-1 and MU 809/7-2 to R.G.).

Supplemental material

Online supplemental material for this paper can be accessed at: http://jp.physoc.org/cgi/content/full/jphysiol.2008.161943/DC1